Understanding the Impact of the Madden-Julian Oscillation and the North Atlantic Subtropical High on Atlantic Tropical Cyclone Variability

A Thesis submitted in partial fulfillment of the requirements for the degree of Master of Science at George Mason University

by

Jacob Campbell
Bachelor of Science
Trinity University, 2011

Director: Natalie Burls, Associate Professor
Department of Climate Dynamics

Summer Semester 2022
George Mason University
Fairfax, VA

DEDICATION

This is dedicated to my loving partner Erin, and my extremely supportive mother, Martha and brother, Sean.

ACKNOWLEDGEMENTS

I would like to thank the many friends, relatives, and supporters who have made this happen. My loving partner, Erin, helped push me to pursue my dreams of obtaining this degree and working in the atmospheric science field. My mom provided support in this department as well. David, Kathy, and Jim were all tremendously helpful in my completion of this and guiding me along the way. Special thanks as well goes to Tim Delsole who helped me with many discussions.

TABLE OF CONTENTS

LIST OF TABLES

LIST OF FIGURES

LIST OF ABBREVIATIONS

ABSTRACT

UNDERSTANDING THE IMPACT OF THE MADDEN-JULIAN OSCILLATION AND THE NORTH ATLANTIC SUBTROPICAL HIGH ON ATLANTIC TROPICAL CYCLONE VARIABILITY

Jacob Campbell, M.S.

George Mason University, 2022

Thesis Director: Dr. Natalie Burls

Tropical cyclone (TC) frequencies in the Atlantic Ocean have multiple influences of variability. Two important ones at subseasonal timescale are the Madden-Julian Oscillation (MJO) and North Atlantic Subtropical High (NASH). A detailed analysis into the combined effects of these together could be helpful in determining higher or lower TC frequencies in the Atlantic subregions – Caribbean, Gulf of Mexico, etc. – and the Atlantic as a whole. An established relationship could also be beneficial for forecasting TCs on a subseasonal timescale. This investigation identifies combinations of this co-relationship utilizing contingency tables and chi-square independence analysis. It is shown there is a possible relationship between MJO and NASH where certain MJO phases modulate the NASH's location and explain some TC frequency patterns. For the Gulf of Mexico, a combination of MJO phases 1-4 and a western NASH extension results in much higher TC counts than expected for a null hypothesis of no MJO/NASH effect.

For the North American east coast, MJO phases 1 through 4 and a northeast NASH extension result in the most TCs. Vertical wind shear values related to MJO phases and observed NASH locations support these findings.

INTRODUCTION

Tropical cyclones (TCs) are a rare and powerful type of storm that can cause catastrophic damage to humans, wildlife, and infrastructure. Although intense TCs can provide extreme winds and rain, which many would believe to be the biggest damage producers, it is storm surge that is often the leading cause of death for TCs affecting the United States (Rappaport, 2014). Tropical cyclones (TCs) tend to form when several factors are favorable including lower wind shear, higher relative humidity, and usually a minimum of 26° (79°F) sea surface temperatures (SSTs) (Gray, 1975). Seasonal variability of TCs in the Atlantic Ocean is strongly related to the occurrence of the El Nino-Southern Oscillation (ENSO) (Lin et al., 2020). El Nino events warm the waters in the tropical Pacific thereby increasing vertical wind shear (VWS) in the Atlantic and suppressing TC activity (Gray, 1984). The eastern Atlantic and Caribbean encompass the Main Development Region (MDR) where 80% of hurricanes and 60% of all named storms develop in the Atlantic. Therefore, any influence on environmental conditions that enhances TC activity in this region is essential to understand. Local SSTs in the North Atlantic can be modulated by many other factors on a seasonal timescale such as the North Atlantic Oscillation (Czaja & Frankignoul, 2002). However, the subseasonal variability, roughly 2-to-6-week timescale, is of great interest regarding prediction and analysis of TCs. This is due to the subseasonal timeframe being deemed a predictability "desert" for all forecasting. There are certain predictable subseasonal atmospheric phenomena that can modulate TCs including the Madden Julian Oscillation (MJO) and the North Atlantic Subtropical High (NASH).

MJO and TCs

Due to the MJO's location in the tropics and several other factors, this oscillation has been shown to effect TC activity with increasing risk of landfalls in North America during specific phases (Vitart, 2009). The MJO is an eastward propagating region of enhanced and suppressed clouds and convection that circles the globe in approximately 30 to 60 days. It has been shown that the MJO is the best predictor of TCs in the Atlantic by an analysis of lead-lag relationships (Camargo et al., 2021). They found that MJO phases with enhanced convection in the Indian ocean increased TC genesis and activity with rising air, convergence, and lower wind shear while enhanced convection in the Western Pacific Ocean near the Philippines correlated with subsidence, divergence, and higher wind shear, resulting in less TC genesis in the Atlantic. A recent study showed that the MJO TC genesis relationship varies for different sub-basins and environmental factors in the Atlantic (Zhao & Li, 2019). Specifically, positive humidity anomalies had the strongest influence on increasing TC genesis numbers during MJO convection present in the central Indian Ocean, while low VWS showed the strongest relationship for genesis in the eastern Atlantic during MJO convection in the central and eastern Indian Ocean. Vitart (2009) showed that the MJO could regulate TC landfalls. With consistent results illustrating TC dependence on the location of the MJO-related convection, this study will also reanalyze MJO’s effects on TC trajectories and frequencies in the Atlantic.

NASH and TCs

Another large-scale climate phenomenon that affects TCs is the North Atlantic Subtropical High (NASH). This robust climatological feature in the sea-level pressure is a local manifestation of the descending branch of the Northern Hemisphere Hadley cell. Variations in its location and size have an impact on the location of a spectrum of atmospheric disturbances. Davis et al., (1997) explored the variability of the NASH from 1899 -1990 using principal component analysis on the spatial variance structure of the NASH. As it fluctuates in strength and location, the NASH can either assist in recurving storms away from the US East coast or help drive them more westward into a landfall scenario. A link to stronger Indian Monsoons causing a stronger NASH, which results in a westward shift in TC activity, has also been examined (Kelly et al., 2018). Additionally, Kelly et al., (2018) postulated that the variation of the NASH is partially correlated with monsoonal intraseasonal variability, but more studies would be required to determine their relation and any TC modulation. Another examination of the influence of NASH on TCs showed that it is the latitudinal location of the NASH, and not its strength, that controls the frequency of landfalling TCs, mainly with storms forming near the Lesser Antilles (Pérez-Alarcón et al., 2021). Figure 1 from Perez-Alarcon et al. 2020 illustrates the basin dependent TC track density with the associated NASH location and strength. There is visual evidence that an east/west motion of the NASH affects landfalling storms. As the western edge of the NASH extends towards North America, this shifts the region of landfalling TCs into the Gulf of Mexico. As NASH becomes more compact and the western edge moves east, this shifts the landfalling TC location to be closer to the east coast of the United States. It is unclear whether the north/south variability, east/west variability, or changes in intensity of the NASH have the largest impact on the frequency of Atlantic TCs or their trajectory. This study investigates the impact of the NASH on TC frequency and tracks.

There have been a number of studies on the linkage of TC frequency, genesis, and/or tracks with either MJO or NASH referenced previously. However, no studies have investigated the combined effect of both on TC frequency and trajectories. This study investigates the impact of the MJO and NASH on TC frequency, and on TC trajectories, in the Atlantic basin.

Subseasonal TC Forecasting

European Centre for Medium-Range Weather Forecasts (ECMWF) model has shown the best skill in forecasting TC frequency and tracks in the North Atlantic basin and many other basins around the world (Lee et al., 2020). Dey et al., (2020) showed that the ECMWF model skillfully predicted MJO out to 31 days. With further MJO forecasting improvements, which strongly affects TCs, an increase in subseasonal TC forecasting seems a likely possibility. However, specific issues have been identified with the ECMWF TC tracks including too short and too quick recurving storms compared to those seen in observations. This study investigates the subseasonal re-forecast tracks that occur in each subregion of the Atlantic. These subseasonal predicted tracks are also investigated in conjunction with both the NASH and MJO to understand their effect on ECMWF predicted storm counts and tracks at different subseasonal forecast lead times.

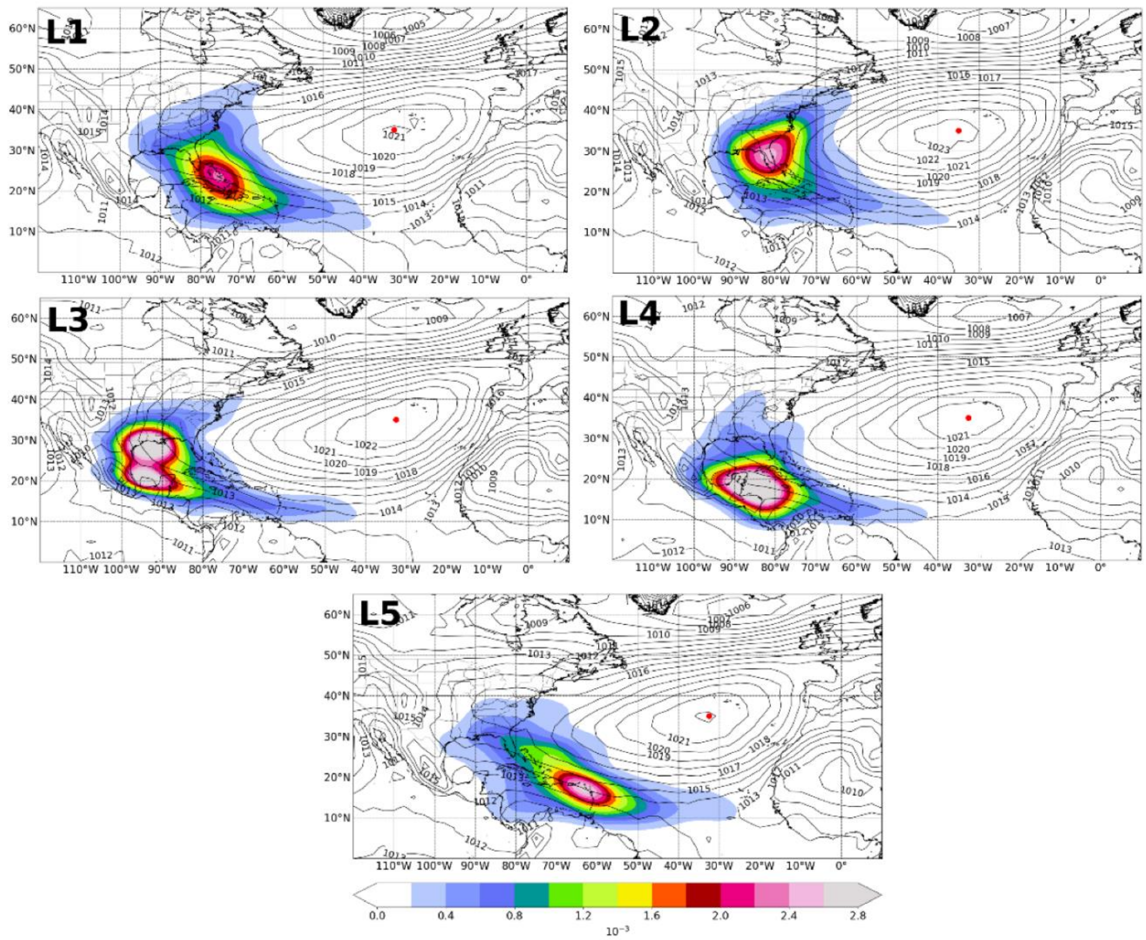

Figure 1: Kernel density estimation (KDE) for the trajectory of TCs that make landfall in each region. Contour lines represent the composite of mean sea level pressure for a specific month and specific year that landfalling events occurred. The red point and LN (N = 1, 2, 3, 4, 5) represents the NASH center and each landfalling cluster, respectively. (from Pérez-Alarcón et al., 2021)

Scientific Questions

The main purpose of this study is to determine if a combination of MJO and NASH produces more or less TC activity in different subbasins of the Atlantic. To reanalyze established associations, per previous literature, relationships between MJO and NASH and related TC frequencies and trajectories for each are investigated. Additionally, does the NASH's position and shape depend on certain phases of the MJO? And does this drive storm counts? For example, inside a grouping of MJO phases, are there certain NASH movements that cause less or more storms to occur? VWS will be able to assist explanation of the storm frequency results pertaining to combinations of MJO and NASH.

DATA AND METHODS

Observed TC Tracks

Historical TCs are extracted from the HURDAT2 best track dataset produced by the National Hurricane Center (Landsea & Franklin, 2013). Along with the track, this dataset includes variables recorded for each storm including maximum surface sustained winds, minimum sea level pressure, 6-hourly central storm location, and wind radii maximum extent. In this study storms categorized as tropical storms or hurricanes are examined. The daily storm latitude and longitude locations for the period 1979-2018 are used for consistency with the available MJO and NASH data. To get a clearer understanding of the different storm frequencies and effects of the MJO/NASH in finer detail, the Atlantic Ocean basin is split into 4 different regions, following Colbert & Soden, 2012. They consist of the Caribbean Sea, Gulf of Mexico (GOM), North America east coast (NA EC), and storms that are not a threat to any major landmass (Out to Sea, OTS) (Figure 2).

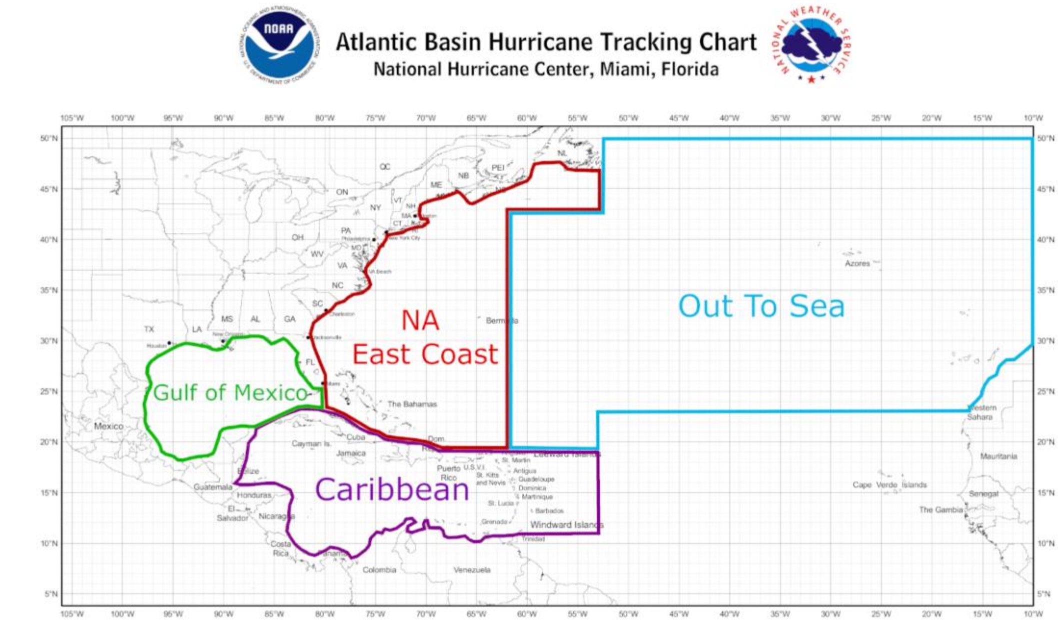

Figure 2: Atlantic subregions with labels overlaying the NOAA official Atlantic Basin Hurricane Tracking Chart courtesy of the NHC (https://www.nhc.noaa.gov/tracking_charts.shtml)

MJO

The MJO is defined using the real-time multivariate (RMM) MJO index (Wheeler & Hendon, 2004). This index is determined based on combined empirical orthogonal functions of observed zonal winds at 200 and 850 hPa and outgoing longwave radiation (OLR). The OLR is a good proxy for precipitation in the tropics, with lower OLR indicating higher cloud tops and hence enhanced convection. The two RMM indices together define a phase and amplitude of the MJO. These observed values are obtained from the Australian Bureau of Meteorology: (www.bom.gov.au/climate/mjo/graphics/rmm.74toRealtime.txt). RMM amplitude values >= 1.0 are used to identify active, or strong, MJO phases (Wheeler & Hendon, 2004). Based on the RMM index, the MJO can be defined by eight phases indicating the location of the enhanced convective activity (Figure 3). For this study, MJO phases 1-4 (MJO1-4), with enhanced convection in the central and eastern portions of the Indian Ocean, are grouped together as more favorable for TC activity and MJO phases 5-8 (MJO5-8), with enhanced convection over Western Pacific, are grouped together as less favorable for TC activity. This grouping is based on results from Vitart (2009), Zhao & Li (2019) and Camargo et al., (2021).

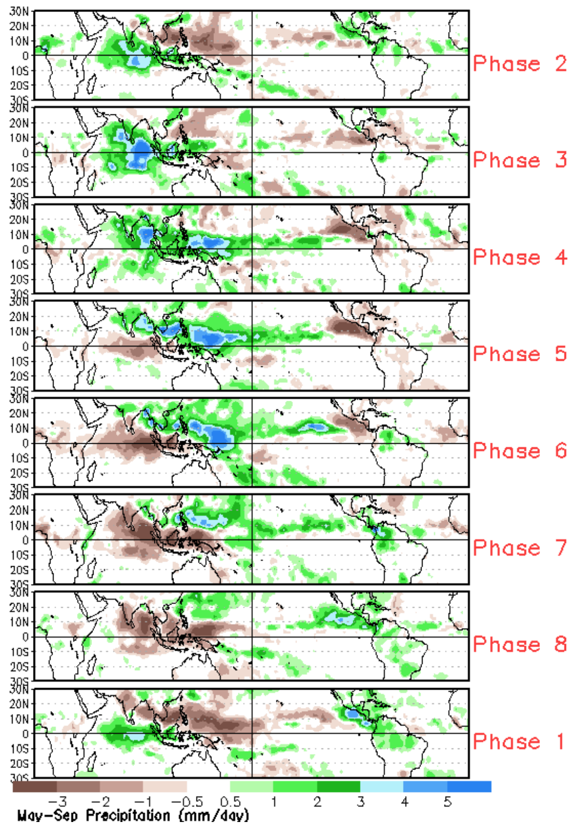

Figure 3. Typical May to September precipitation composite maps for region where MJO propagates in the tropics. All eight phases are shown with Phase 1 starting at the bottom plot. Enhanced precipitation in green and blue, suppressed precipitation in browns.

NASH

The daily variability and strength of the NASH are determined following Li et al., (2011). The movement of the NASH's western ridge, or boundary, which extends toward North America from the Atlantic, is quantified relative to the climatological latitude and longitude of the location of the furthest western point of the ridge (~78°W, ~32°N) over the years 1979-2018. This ridge line location is determined by 1) a change in the zonal winds from easterlies to westerlies where $u = 0$, and 2) the zonal wind gradient with respect to latitude greater than 0, or $\partial u/\partial y > 0$. The 1,560 gpm isoline is used to represent the outermost boundary of the NASH following Li et al., (2011). This allows the western ridge location to be specified by the intersection of the isoline and the calculated ridge line meeting the criteria above. With these daily latitude and longitude locations, a quadrant system, with the climatological mean position of NASH as the origin and the cardinal directions as the axes, is utilized, again as in Li et al., (2011). Each daily western ridge location is assigned in either the NE, NW, SW, or SE quadrant. A visual representation of the four variations of NASH's western ridge can be seen in Figure 4. Figure 5 shows how the NASH location can shift away from the climatological center point into any quadrant.

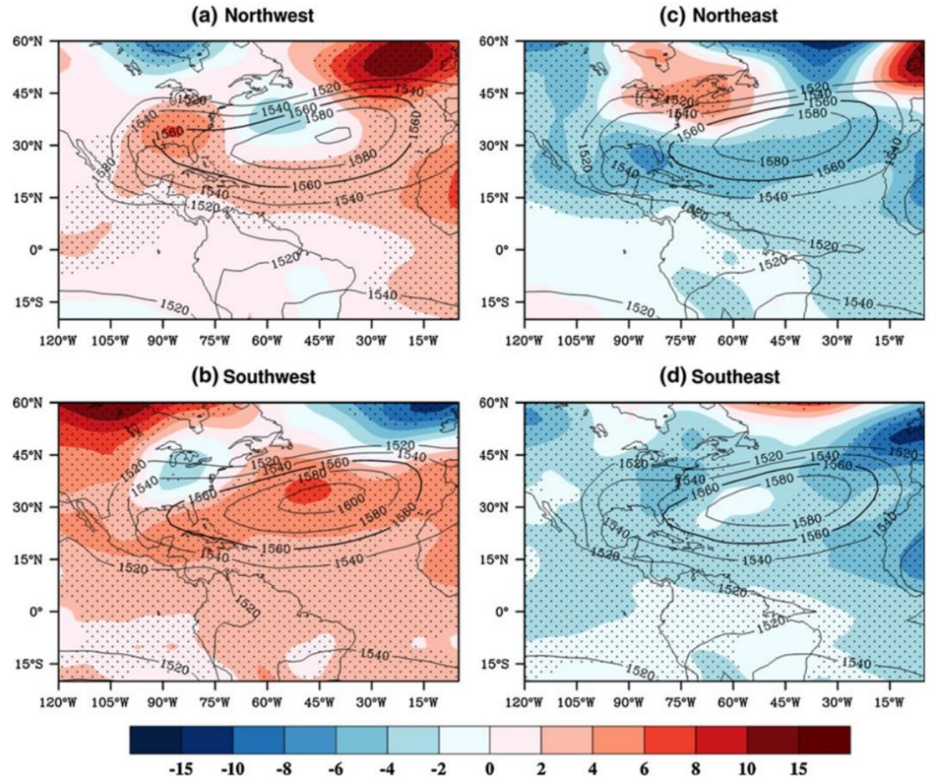

Figure 4. Average NASH spatial shape for each NASH quadrant location taken from Li, et al. (2012). Color contours represent 850 hPa geopotential height anomalies. Contour lines indicate height levels with the 1,560 GPM isoline bolded.

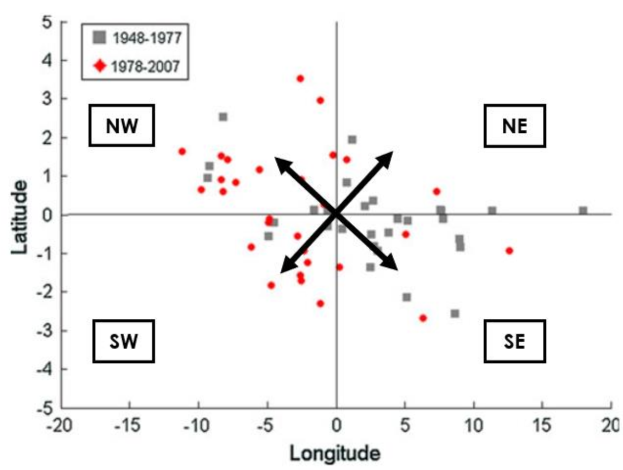

Figure 5. Overlayed quadrant labels and arrows of the spatial distributions of the NASH western ridge relative to its climatological mean position during 1948-1977 (gray squares) and 1978-2007 (red diamonds). Taken from Li et al., (2011)

VWS and Geopotential Height Fields

To understand how the MJO and NASH impact TC storm counts, VWS is calculated from the daily ERA-Interim reanalysis (Dee et al., 2011) product (0.75° x 0.75°) as the difference between the 200 hPa and 850 hPa zonal wind. The ERA-Interim geopotential height at 850 hPa is also used to understand how the variability of the NASH impacts storm frequencies.

METHODS

Contingency Tables and Chi-Square Tests

To quantify the significance of MJO/NASH and TC relationships, a chi-squared test of independence is used with a 5% significance level (p values <= .05). Utilizing 2x2 contingency tables, storm counts are quantified for specific Atlantic basin subregions, MJO1-4/MJO5-8, and NASH North/South or NASH East/West western ridge locations. For each region, a significant p value indicates a detectable dependence of storm counts on a combination of MJO and NASH categories. P values greater than .05, but still relatively low, will be analyzed as well to identify possible relationships that cannot be detected as significant given the sample size of the dataset. The significance of the relationship between 1) MJO + TC counts, 2) NASH + TC counts, and 3) MJO/NASH + TC counts for all subregions are evaluated using the chi-square test of independence.

An example contingency table is shown in Table 1. Figure 6 shows the same information in an alternate format called a mosaic plot. A mosaic plot is a way to visualize the contingency table where larger cells signify a larger percentage of the sample. The cells that are colored red or blue correlate with Pearson residual values which are a measure of how much an observed value or storm count is different than the expected value, or storm count, under a null hypothesis of independence. The larger (smaller) these values, the more likely they are to appear blue (red). The cells that indicate a larger departure from independence signify a possible relationship between the MJO/NASH and storm counts (or days). Pearson residuals mathematically are equivalent to $\frac{\text{Observed} - \text{Expected}}{\sqrt{\text{Expected}}}$.

Table 1: Sample 2x2 Contingency Table

Region or Combination of Regions			
NASH/MJO	MJO1-4	MJO5-8	Totals
North	counts	counts	
South	counts	counts	
Totals			

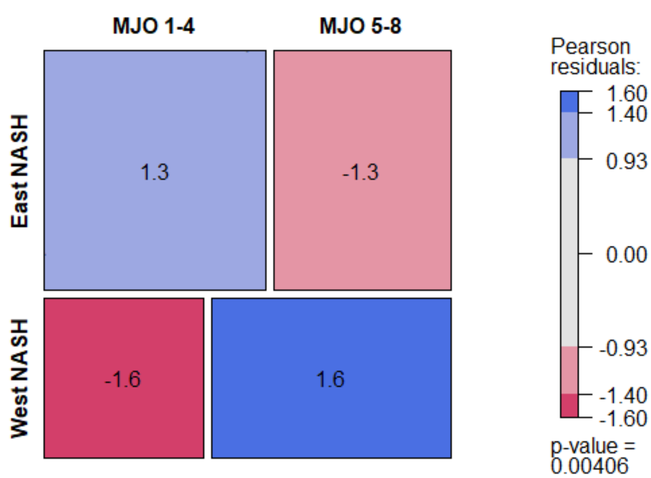

Figure 6: Example mosaic plot with sample MJO and NASH categories. Pearson residual scale shown on right along with p-value from chi-square significance test.

Environment Maps

Maps showing VWS and geopotential height are used to provide a physical explanation for relationships between MJO/NASH and TC storm counts or days. They indicate a more or less favorable environment for storm counts than anticipated given a certain category of MJO or NASH.

Subseasonal Tracks

Finally, an exploratory analysis of the forecasted tracks and TC frequencies from the ECMWF model is performed. The model TC frequencies are compared with observed frequencies to determine if the model can identify shifts in TCs related to MJO phase and NASH western ridge locations.

RESULTS

Impact of the MJO on TC Storm Counts

This study first investigates the storm counts for the four TC regions during favorable (1-4) and unfavorable (5-8) MJO phases (Figure 7). More TCs occur during MJO 1-4 phases than MJO 5-8 in all regions. This asymmetry is largest in the Caribbean and Gulf of Mexico (GOM), where storms during MJO 1-4 phases outnumber storms during MJO 5-8 more than 2:1. This is consistent with previous studies (Camargo et al., 2021; Vitart, 2009; Zhao & Li, 2019). To gain more insight into the causes of this difference, the VWS in the Atlantic during the favorable and unfavorable MJO phases is investigated (Figure 8). During MJO 5-8 phases, higher VWS than in MJO 1-4 phases can be seen in the MDR. This confirms the results from past studies that determined low VWS in this area contributed to increasing TC activity (Zhao & Li, 2019). A chi-square test of independence indicates a significant relationship between MJO phase and TC storm counts in each subregion.

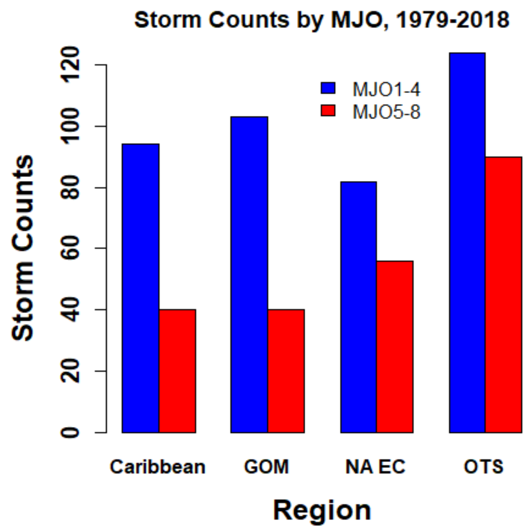

Figure 7. Bar plot showing the MJO phases split into their respective categories including for the four separate subregions of the Atlantic (Caribbean, GOM = Gulf of Mexico, NA EC = North American East Coast, and OTS = Out To Sea). Y-axis shows total storm counts for specific MJO category and subregion.

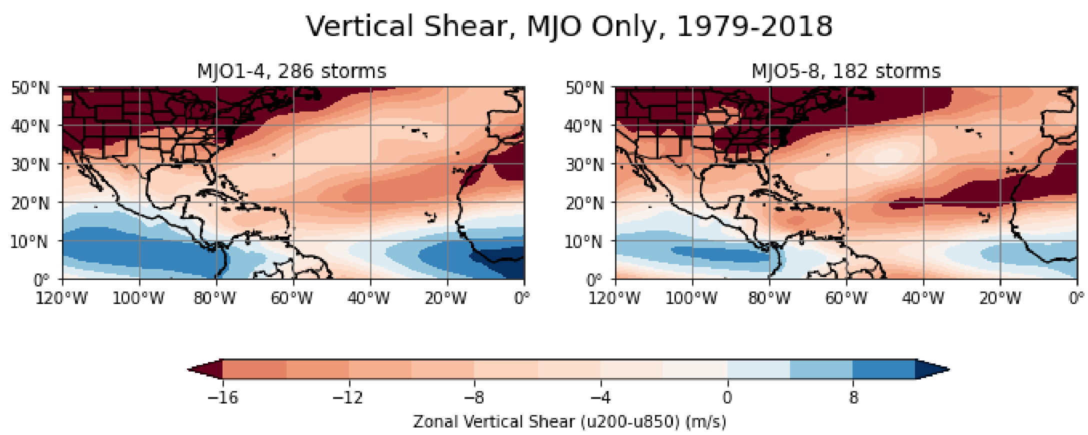

Figure 8. Shear comparison map showing zonal VWS values for the two MJO categories. This is for all storms for the Atlantic. Total storms are also noted for each category. The red dotted box indicates the Main Development Region.

Impact of the NASH on TC Storm Counts

The bar plot in Figure 9 shows the storm counts for each subregion for the four NASH categories. The northwest extension of the NASH produces the most TC activity in all regions. The southwest NASH position produces the second most TCs in the Caribbean, GOM, and NA EC. This indicates that a western shift of the NASH produces more TC activity than an eastern shift of the NASH in these regions. The associated geopotential height composites for each quadrant of the NASH are shown in Figure 10. When the NASH is shifted northwest and southwest, an elongated band of high pressure extends westward into the mainland of the US. When the NASH is shifted northeast and southeast, high pressure is retracted away from the US mainland into the Atlantic Ocean so that the overall NASH is much more compact. The Out to Sea region of the Atlantic has a much higher number of storms for the eastern NASH locations than do the other regions (Figure 9). The retracted western ridge into the Atlantic Ocean allows storms to easily curve around the western periphery of the NASH and not affect any major landmasses. The relationship for NASH locations and storm counts are significant based on a chi-square test of independence. There does not appear to be a difference in overall NASH intensity between the four NASH locations.

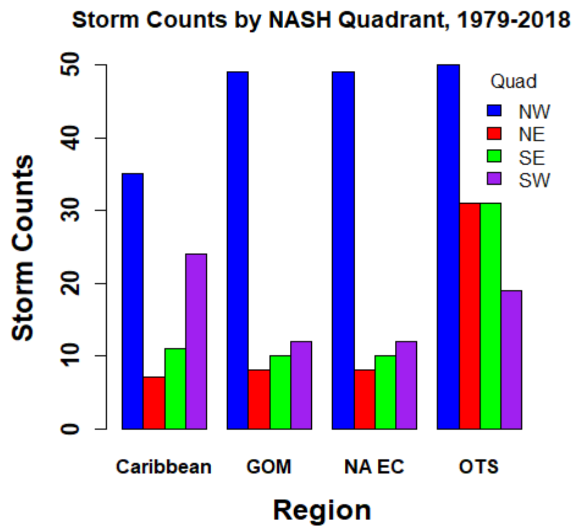

Figure 9. Bar plot showing NASH quadrant locations the western ridge is in along with the four subregions of the Atlantic (Caribbean, GOM = Gulf of Mexico, NA EC = North American East Coast, and OTS = Out to Sea). X-axis is total storm counts for each NASH quadrant location.

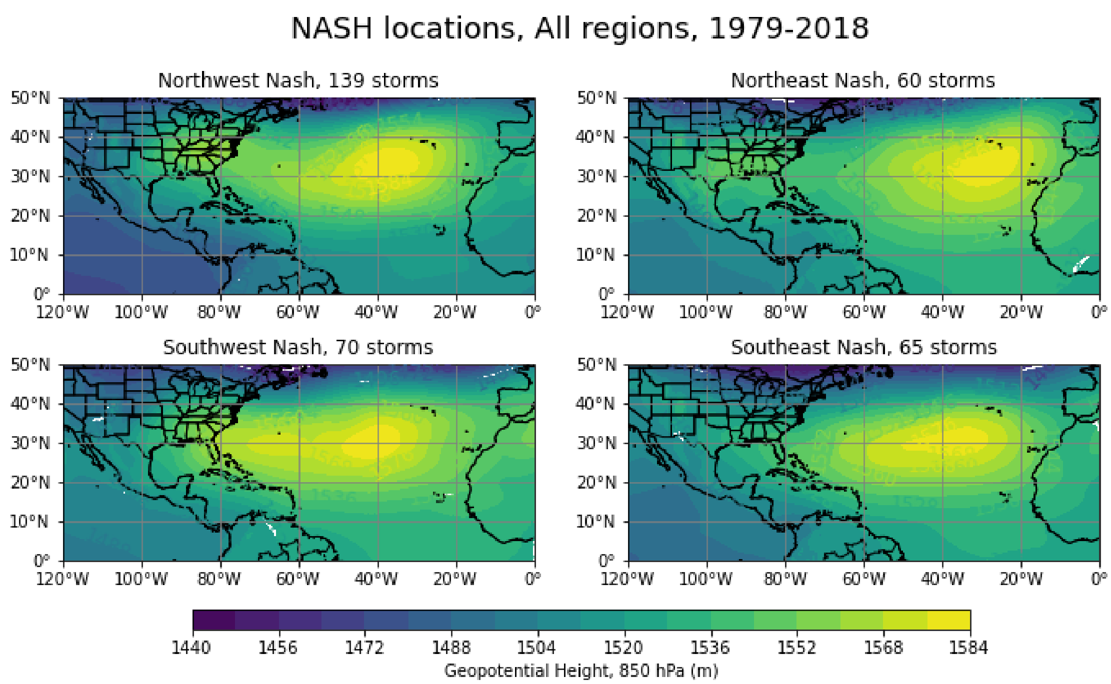

Figure 10. Geopotential height comparison map showing the four different NASH western ridge extensions or retractions for the four quadrant locations. Total storms are also noted for each category.

Are the MJO and NASH Related?

Before investigating storm counts for the combination of NASH and MJO categories, it is important to understand if the frequency of occurrence of NASH and MJO are independent from each other or if there is a relationship between them. The number of days in each combination of MJO phase and NASH location category is quantified (Figure 11). MJO 1-4 phases in conjunction with a southward shift of the NASH occurs significantly more often than any of the other categories (Figure 11, left). This shows a strong preference for the NASH to have a southern extension during the MJO1-4 phases. During MJO phases 5-8, there is a strong preference for the NASH to be shifted westward rather than eastward (Figure 11, right).

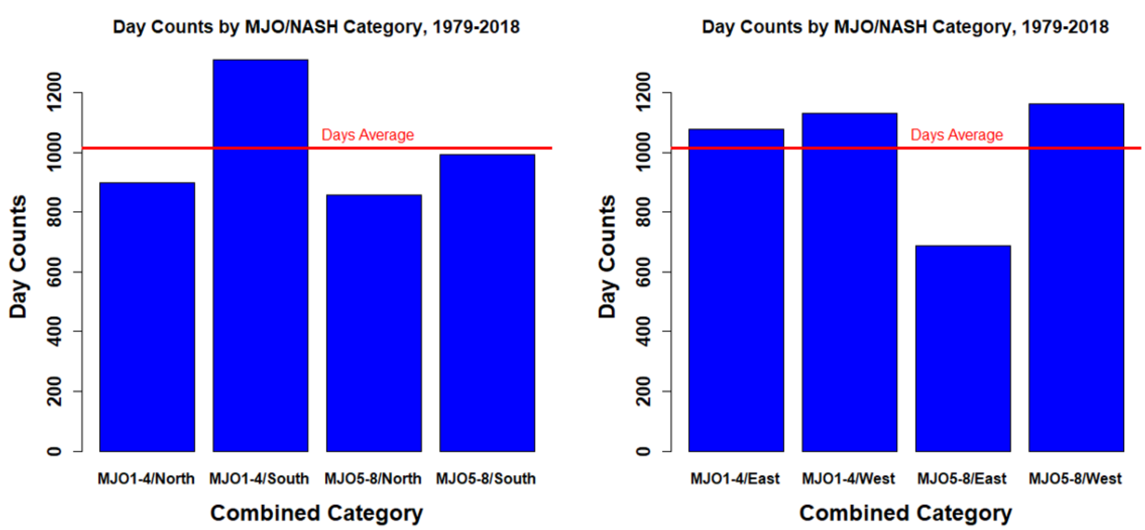

Figure 11. Bar plots showing the frequency of simultaneous days occurring between the two MJO categories and two NASH categories. Left plot shows MJO relation with North and South NASH locations. Right plot shows the same relation but with East and West NASH locations.

A chi-square test of independence shows a strong mirrored diagonal relationship for both NASH categories seen in the associated mosaic plots (Figure 12). The p value is small for east and west NASH locations indicating a relationship with the MJO phase categories. For north and south NASH locations, the differences are significant at the 5% level indicating a relationship between MJO and NASH locations as well. As this relationship is initially assumed to be independent, this unequal distribution of sample size of days in each could impact storm counts when investigating the combined impact of the MJO and NASH.

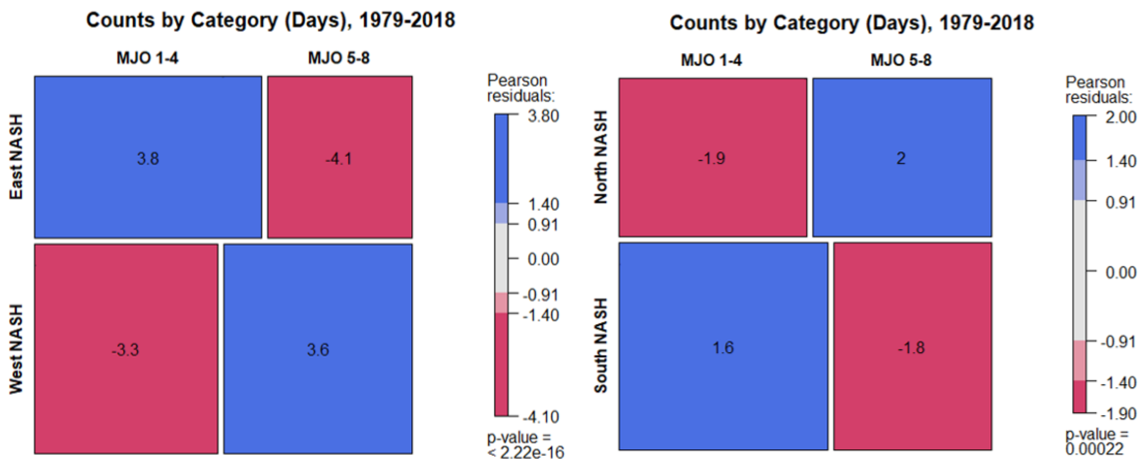

Figure 12. Mosaic plots for the associated day frequencies for the two MJO categories with (left) NASH east and west locations and (right) NASH north and south locations. Pearson residual values are color coded, and values labeled for each individual cell. P values are also listed for the chi-square independence test.

The Combined Impact of the MJO and NASH on TC Storm Counts

Caribbean

The individual impact of the MJO and NASH on TC storm counts and the relationship between the MJO-NASH have been established in the previous sections. This section investigates TC storm counts for combinations of the NASH and MJO. The only region for which a significant relationship was found is the Caribbean. Table 2 shows the raw results in the contingency table along with the associated mosaic plot in Figure 13. For an eastward NASH movement, fewer storms are seen during MJO phases 5-8 compared to the expected number under an assumption of independence. When the NASH shifts westward, more storms occur than expected indicating a relationship between TC activity and NASH location during MJO phases 5-8. This relationship is not unexpected as the least number of storms is associated with the least number of days and the greatest number of storms in MJO5-8 occurred with the higher number of days (Figure 12). However, the ratio of days occurring in MJO phases 1-4 versus in MJO phases 5-8 is ~1.2:1 while the ratio of storms occurring in MJO1-4 versus MJO5-8 is ~2:1. This suggests that there could be other factors in play besides a simple sample size preference for the storms to form.

Table 2. TC counts for Caribbean, east/west NASH, 1979-2018

Caribbean			
NASH/MJO	MJO1-4	MJO5-8	Totals
East	33	5	38
West	27	17	44
Totals	60	22	160

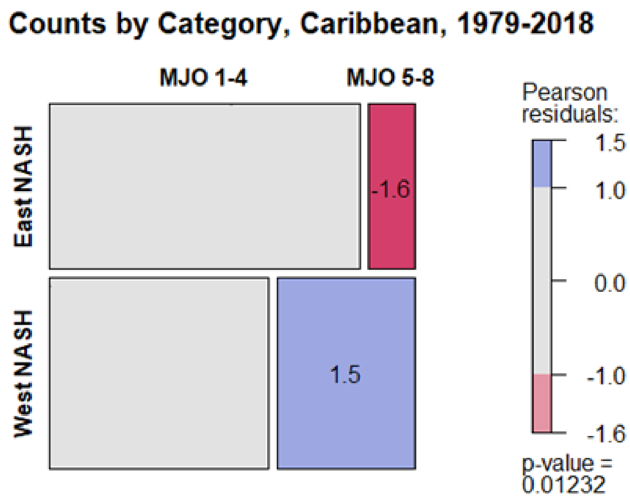

Figure 13. Associated mosaic plot for the 2x2 contingency table seen in Table 2 for the Caribbean region and an east/west NASH location

These results are further investigated using composites of VWS for the combinations of MJO and NASH categories along with the NASH position (Figure 14). A western extension of the NASH results in more storms overall (that is, independent of the MJO) than does an eastward extension. However, the highest storm count for an individual category occurs when the NASH is shifted eastward and the MJO is in phase 1-4. This seems counterintuitive as the eastern retraction of the NASH would allow more storms to move northward and possibly move along the NA EC rather than enter the Caribbean. However, the VWS shows that the MDR region has the lowest values of all four categories during MJO1-4 phases and eastward shifted NASH (Figure 14, upper left). The highest VWS is seen during MJO phases 5-8 and eastward shifted NASH which corresponds to the lowest storm totals (Figure 14, upper right). During MJO phases 5-8, there is lower VWS in the MDR region when the NASH is shifted westward, providing an explanation for 3 times the storm counts compared to an eastward shift of the NASH during the same phases of the MJO.

Finally, a metric of storms per day is shown in the bottom left of each subplot in Figure 14. This is a calculation taking the number of storms for a specific MJO and NASH category and dividing that by the number of days in that combination from Figure 11. If the number of days is the driver of storm counts, these values should be the same or similar. However, The MJO 1-4 storm per day counts are much higher than the MJO 5-8. This indicates that a physical relationship such as lower VWS is more likely the reason for increasing storm counts than sample size. The same comparison is performed between north and south NASH movements during different phases of the MJO and a preference for higher storm counts is found during a northern shift of the NASH (not shown). However, this difference is much smaller than for east-west shifts of the NASH.

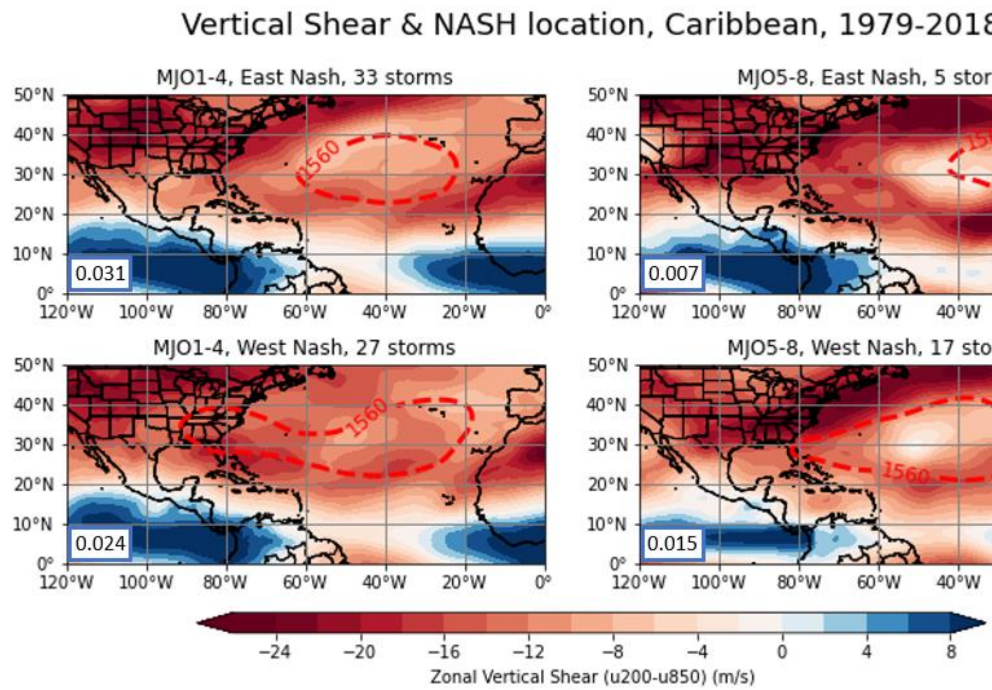

Figure 14. Average VWS for the Caribbean storms occurring for the four different combinations of MJO and NASH east/west categories. NASH location is indicated by the dotted red closed contour line which corresponds to the 1,560 GPM isoline, or the boundary of the NASH. Blue outlined numbers in the bottom left are storms per days.

Gulf of Mexico

The GOM and NA East Coast are the other two regions investigated. Here TCs can have the most impact due to their proximity to the US coastline and potential for landfall. Although these two regions did not show statistically significant relationships between the MJO, NASH, and TC counts, there is evidence of preferences for different phases and evidence of physical relationships. A significant relationship is not detectable, likely due to small sample sizes. The most storms occur when the NASH is shifted west and when MJO is in phases 1-4 (Figure 15, bottom left). This is an expected result as the NASH needs to extend further west than the Caribbean to drive potential TCs into the GOM.

Consistent with the storm counts, there is nearly zero shear during MJO phases 1-4 and westward shifted NASH while there is higher shear during MJO 5-8 and eastward shifted NASH (Figure 15, upper right). As almost all storms that develop are moving westward into the Caribbean, VWS values here and eastward in the MDR are very influential in assisting in the development of storms or suppressing activity. During MJO phases 1-4, there is slightly more VWS in the GOM itself when the NASH is shifted eastward than westward with much lower shear values in the Caribbean. As many storms that develop in the Caribbean move into the GOM, it is reasonable to expect that low shear values in the Caribbean would result in more storms in the GOM. For the storms per day calculation, the values are consistent in magnitude and difference for the four categories, following those trends seen for the Caribbean results. This is not a surprise since the GOM and Caribbean are neighbors to each other and often pass off storms to one another as well. Consistent with the results in the Caribbean, a northern shifted NASH results in a higher storm favorability in the GOM, but an east/west NASH shift has a larger impact.

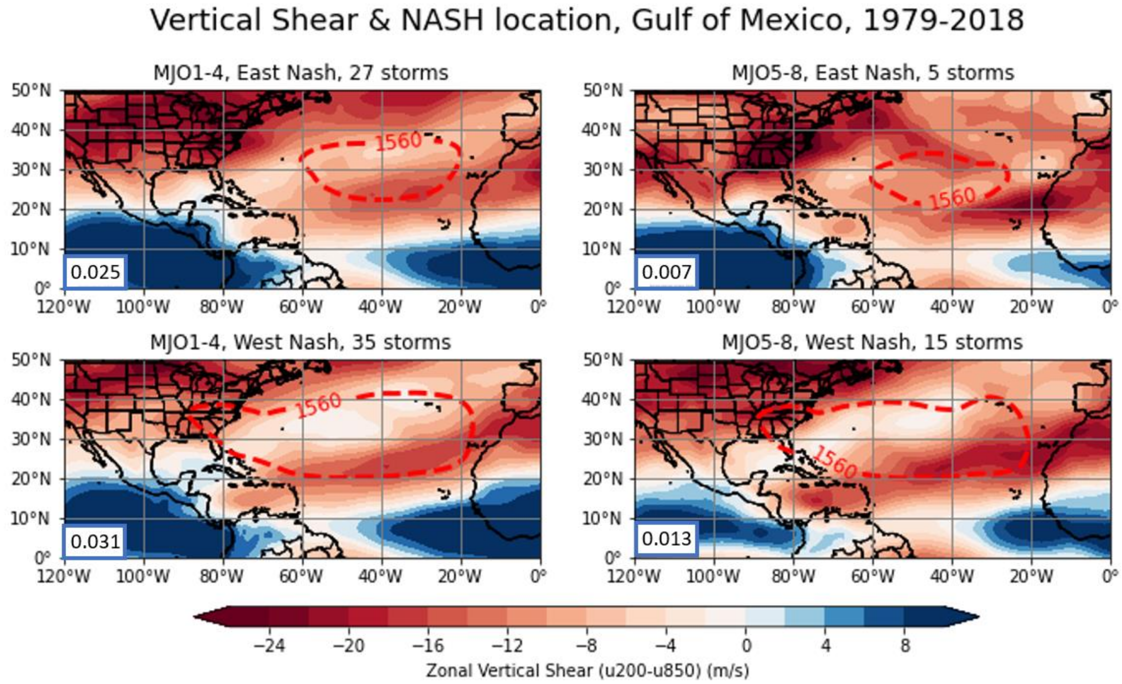

Figure 15. As in Figure 14 but for the Gulf of Mexico.

North American East Coast

The North American east coast subregion contains storms that are a threat to make landfall anywhere along the US and Canadian coasts. Following the previous results, the east and west NASH locations and north and south NASH locations are investigated. A north and south NASH location shows some differences between storm number and day frequency between MJO and NASH.

In Figure 16, the east and west shifts of the NASH are visualized. An eastward NASH movement overall results in more storms near the east coast. The impact of the MJO on storm counts is less important in this region than the NASH. The storms per day metric supports this as the two highest values correspond to the eastern NASH categories. This is consistent with how the NASH steers TCs. A westward NASH acts like a blocking high pressure that does not allow storms to turn northwest and north when coming from the MDR. The storms per day for MJO 5-8 phases and eastern NASH is nearly three times the value of the Caribbean and GOM regions despite the low total number of days in this category. The VWS values follow the MJO categories once again with the highest values occurring in the MJO 5-8 phases, especially in the MDR region. There is not a big difference in VWS near the east coast but the storms that end up in this region most likely form in the MDR and Caribbean and then move northward, so the shear immediately near the east coast has less of an effect on an already developed storm moving into this region.

The storm counts in this region and shear values for a north and south shift of the NASH are shown in Figure 17. The highest storm count is evident in the MJO1-4 phases and for the northern NASH location. This combination also results in the highest number of storms per day of the three regions studied thus far. An enhancement in the number of TCs associated with a northern shift of the NASH does make sense as this shift would allow storms more of a chance to turn northward sooner than if that boundary was further south. MJO 1-4 phases and south NASH location tied for the lowest number of storms of the four combinations. However, this combination resulted in the highest number of days resulting in a very low storms per day number. VWS is not dissimilar from the MJO 1-4 phases and North NASH, so a northern NASH position appears to be the driver of the higher storm counts. The VWS differences between the two MJO1-4 categories do not tell the story of this discrepancy so there could be some other environmental conditions not examined that affect the storms in this region beyond NASH position.

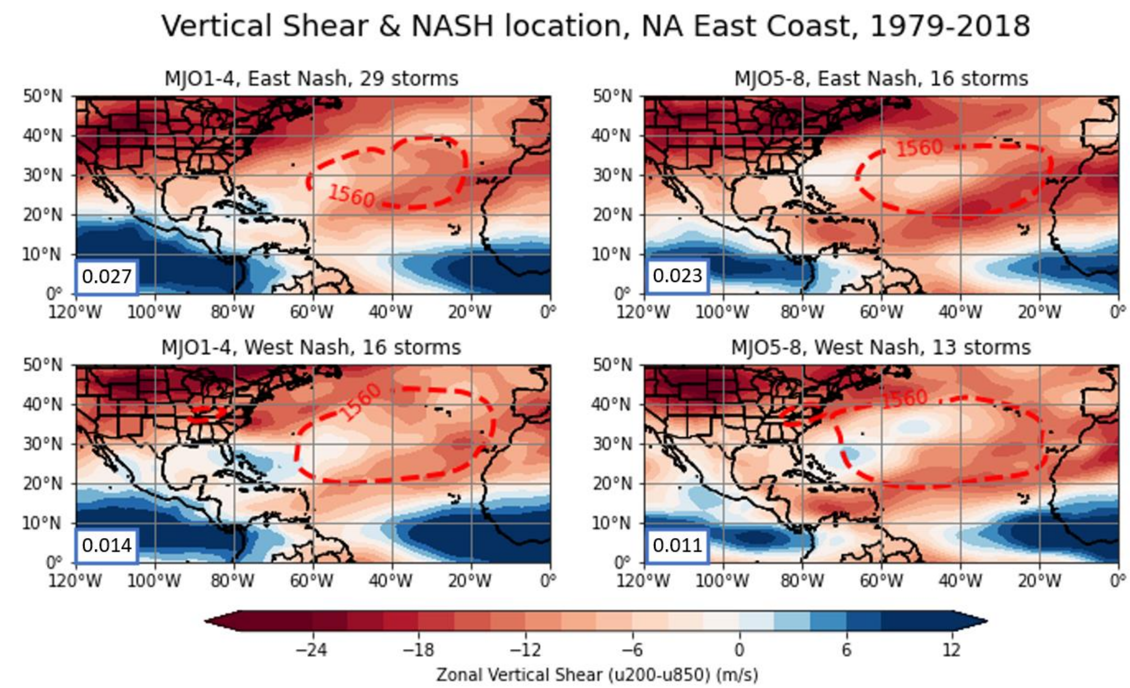

Figure 16. As in Figure 14 but for the North American east coast.

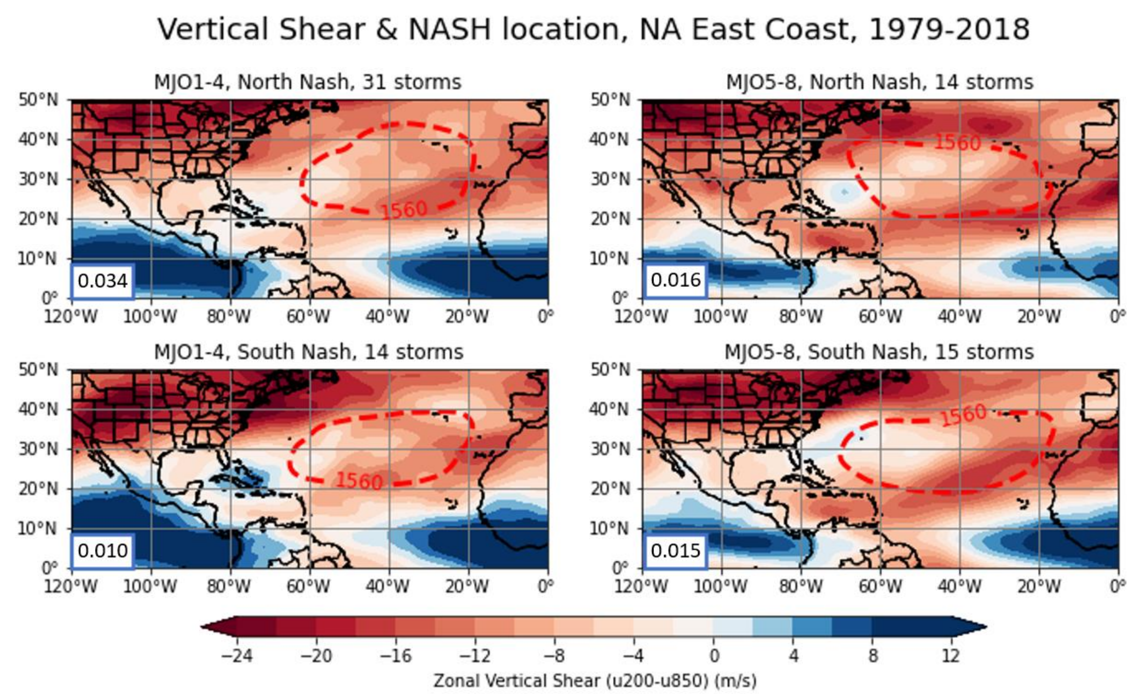

Figure 17. As in Figure 16 but for north/south NASH locations.

Out to Sea

The Out to Sea storms (not shown) show very similar patterns to the NA East Coast region with a preference for a northern and eastern NASH location. Shear differences also follow along MJO1-4 (less VWS) and MJO5-8 (more VWS) lines. As these are neighboring regions as well, this makes logical sense.

DISCUSSION

All Regions

When all storms and regions are combined, the results are averages of the tendencies seen in Figures 14 through 17. The VWS composites for all regions are shown in Figure 18 and 19. The most storms occur in the MJO 1-4 phases and a north and east NASH position. This seemingly conflicts with the overall storm numbers shown for the NASH-only analysis (Section 4b). However, a MJO amplitude threshold of >= 1.0 is used and no similar filtering is applied to the NASH, it would seem removing those storms due to the MJO threshold removed a lot more western NASH location days. This could indicate that the NASH is in a more western location when the MJO is not active. Further study would be required to see why an inactive MJO is associated with a more western shift of the NASH. VWS values are again split by MJO phase with lower values in MJO 1-4 resulting in more storms and higher values in MJO 5-8, resulting in less storms.

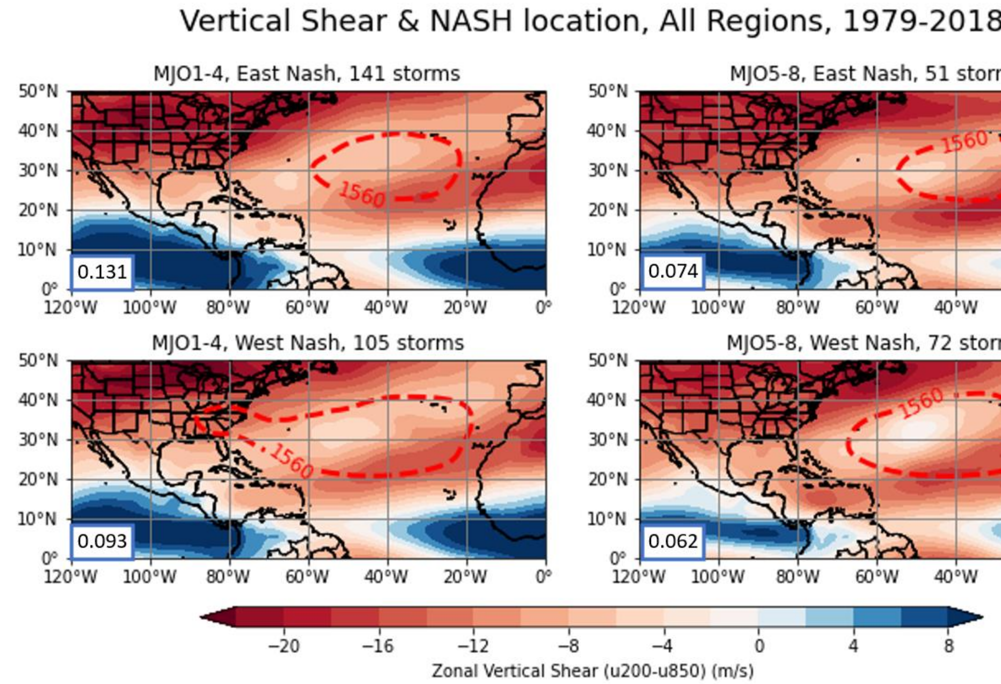

Figure 18. As in Figure 14 but for All Regions.

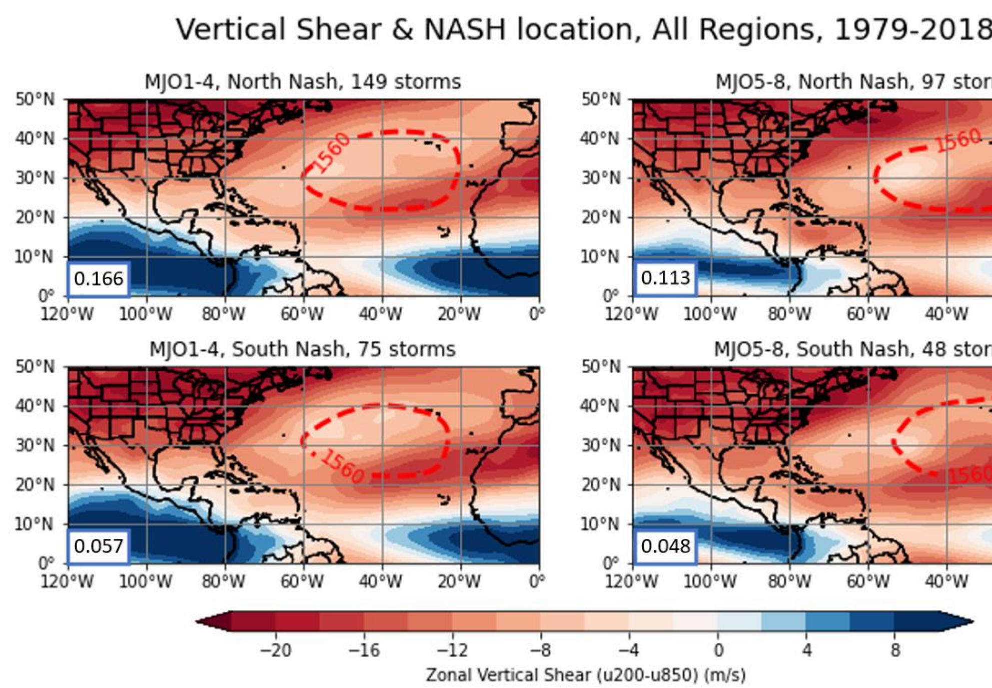

Figure 19. As in Figure 18 but with north/south NASH locations.

For the storms per day values, a smaller spread, between maximum and minimum values, is seen for east/west NASH locations than for north/south. This could indicate a possible stronger relationship between storm counts and north/south NASH locations when taking all regions into account. The storm per day counts that are most noteworthy are the ones relating to the anomalously low and high day counts for the MJO/NASH categories: 0.074 for the MJO5-8/East (lowest days) and .057 for MJO1-4/South (highest days).

All this information taken together suggests that the day counts are not the only factor driving the storm counts. VWS comes into play when considering MJO 1-4 / MJO 5-8 differences. For larger storm differences between NASH categories (like north/south), VWS does not appear to be the only factor modulating TC activity. It is possible other environmental factors could be causing this NASH storm preference (e.g., SSTs, relative humidity, or a combination of both). Further study into this could provide insight into the NASH storm frequency favorability, especially for the north/south NASH locations.

Subseasonal TC Forecasts

Shifting to subseasonal TC prediction, the same methodologies of organizing storms into MJO/NASH combinations is applied to the ECMWF model at different lead times to identify if the model can capture the MJO and NASH preferences for storm counts. Figure 20 shows the results comparing the model storm counts versus observed storm counts. The blue bar indicates observed counts and the colored bars stacked alongside to the right indicate the storm counts for different lead times of the ECMWF model forecasts. At 7 days, the storm counts have a larger drop off than expected. This is due to the observed storm counts including storm tracks that are beyond one week which allows them to move into different NASH locations and/or MJO phase categories throughout its lifetime and allowing it to count twice for two different categories. The model analysis, however, cuts off tracks at the 7th day which would explain this difference in number of storms. Next, an increasing lead time leads to a decrease in storm counts. However, the model can identify the shift in storm counts between MJO phase with the two MJO1-4 phase categories having the highest and MJO5-8 having the lowest. Future work will explore the ability of the model to represent the combined NASH/MJO relationship.

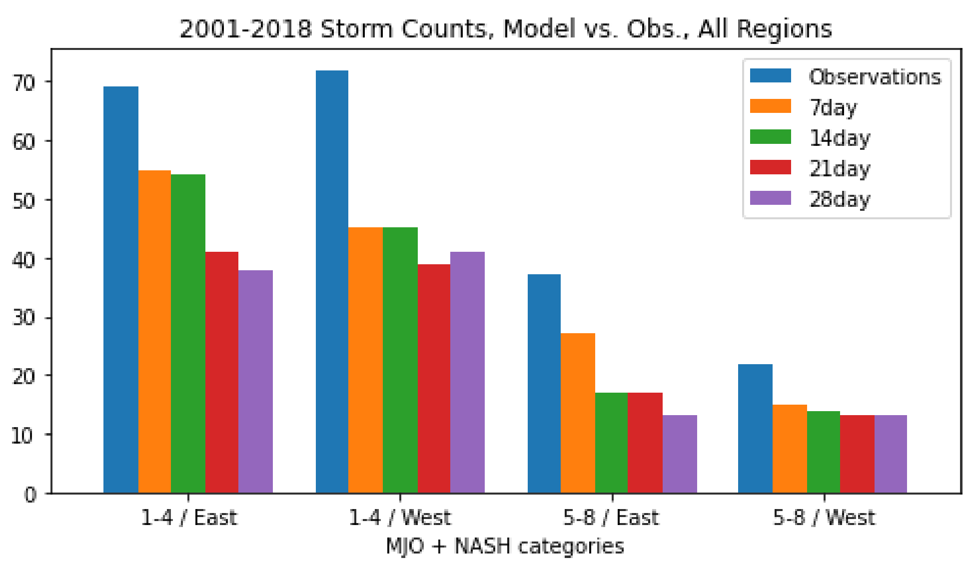

Figure 20. Storm counts for selected MJO and NASH categories, observations vs. model.

Future Work

The relationship between the NASH and MJO identified in observations (Are the MJO and NASH Related?, pg. 20) indicates that the MJO phase could impact the NASH position. Further studies would be beneficial to confirm or refute this relationship. This will be explored in future work.

Placing a threshold on MJO amplitude effectively removed ~50% of all the storms in this study. A more robust examination of the MJO/NASH and TC relationship could include a multiple regression scheme with continuous rather than categorical MJO and NASH definitions that could allow all the days and TCs to be utilized.

CONCLUSION

In this study, the relationships among MJO, NASH, and TC frequencies in the Atlantic, broken down into subregions, were examined. A simultaneous relationship between MJO phase and NASH displacement was found indicating that MJO phases 1-4, with enhanced convection in the central and eastern Indian Ocean, are associated with eastward and southward shifts of the NASH, and MJO phases 5-8, with enhanced convection in the western Pacific Ocean, are associated with westward and northward NASH shifts. The relationship between MJO phase and NASH displacement produces similar asymmetries in TC frequency in some of the sub-regions; however, 1-4 MJO phases were found to strongly modulate VWS, consistent with its relationship with TC frequency. MJO phases 1-4 are related to lower VWS and higher TC frequency. Displacements of the NASH are also strongly related to TC frequencies, depending on the sub-region. The Caribbean and GOM showed strong preference for a western NASH location while the NA east coast showed a strong preference for both north and east NASH locations. Future studies could provide further insight into this MJO/NASH relationship, its effect on storm counts, and how this could improve future TC subseasonal forecasting.

REFERENCES

Camargo, Suzana J., Frédéric Vitart, Chia-Ying Lee, and Michael K. Tippett. “Skill, Predictability, and Cluster Analysis of Atlantic Tropical Storms and Hurricanes in the ECMWF Monthly Forecasts.” Monthly Weather Review 149, no. 11 (November 1, 2021): 3781–3802. https://doi.org/10.1175/MWR-D-21-0075.1.

Colbert, Angela J., and Brian J. Soden. “Climatological Variations in North Atlantic Tropical Cyclone Tracks.” Journal of Climate 25, no. 2 (January 15, 2012): 657–73. https://doi.org/10.1175/JCLI-D-11-00034.1.

Czaja, Arnaud, and Claude Frankignoul. “Observed Impact of Atlantic SST Anomalies on the North Atlantic Oscillation.” Journal of Climate 15, no. 6 (March 15, 2002): 606–23. https://doi.org/10.1175/1520-0442(2002)015<0606:OIOASA>2.0.CO;2.

Davis, Robert E., Bruce P. Hayden, David A. Gay, William L. Phillips, and Gregory V. Jones. “The North Atlantic Subtropical Anticyclone.” Journal of Climate 10, no. 4 (April 1, 1997): 728–44. https://doi.org/10.1175/1520-0442(1997)010<0728:TNASA>2.0.CO;2.

Gray, William M. “Atlantic Seasonal Hurricane Frequency. Part I: El Niño and 30 Mb Quasi-Biennial Oscillation Influences.” Monthly Weather Review 112, no. 9 (September 1, 1984): 1649–68. https://doi.org/10.1175/1520-0493(1984)112<1649:ASHFPI>2.0.CO;2.

Kelly, Patrick, L. Ruby Leung, Karthik Balaguru, Wenwei Xu, Brian Mapes, and Brian Soden. “Shape of Atlantic Tropical Cyclone Tracks and the Indian Monsoon.” Geophysical Research Letters 45, no. 19 (2018): 10,746-10,755. https://doi.org/10.1029/2018GL080098.

Landsea, Christopher W., and James L. Franklin. “Atlantic Hurricane Database Uncertainty and Presentation of a New Database Format.” Monthly Weather Review 141, no. 10 (October 1, 2013): 3576–92. https://doi.org/10.1175/MWR-D-12-00254.1.

Lee, Chia-Ying, Suzana J. Camargo, Fréderic Vitart, Adam H. Sobel, Joanne Camp, Shuguang Wang, Michael K. Tippett, and Qidong Yang. “Subseasonal Predictions of Tropical Cyclone Occurrence and ACE in the S2S Dataset.” Weather and Forecasting 35, no. 3 (June 1, 2020): 921–38. https://doi.org/10.1175/WAF-D-19-0217.1.

Li, Laifang, Wenhong Li, and Yochanan Kushnir. “Variation of the North Atlantic Subtropical High Western Ridge and Its Implication to Southeastern US Summer Precipitation.” Climate Dynamics 39, no. 6 (September 2012): 1401–12. https://doi.org/10.1007/s00382-011-1214-y.

Lin, I-I, Suzana J. Camargo, Christina M. Patricola, Julien Boucharel, Savin Chand, Phil Klotzbach, Johnny C. L. Chan, et al. “ENSO and Tropical Cyclones.” In El Niño Southern Oscillation in a Changing Climate, 377–408. American Geophysical Union (AGU), 2020. https://doi.org/10.1002/9781119548164.ch17.

Pérez-Alarcón, Albenis, José C. Fernández-Alvarez, Rogert Sorí, Raquel Nieto, and Luis Gimeno. “The Combined Effects of SST and the North Atlantic Subtropical High-Pressure System on the Atlantic Basin Tropical Cyclone Interannual Variability.” Atmosphere 12, no. 3 (March 2021): 329. https://doi.org/10.3390/atmos12030329.

Rappaport, Edward N. “Fatalities in the United States from Atlantic Tropical Cyclones: New Data and Interpretation.” Bulletin of the American Meteorological Society 95, no. 3 (March 1, 2014): 341–46. https://doi.org/10.1175/BAMS-D-12-00074.1.

Vitart, F., J. L. Anderson, and W. F. Stern. “Simulation of Interannual Variability of Tropical Storm Frequency in an Ensemble of GCM Integrations.” Journal of Climate 10, no. 4 (April 1, 1997): 745–60. https://doi.org/10.1175/1520-0442(1997)010<0745:SOIVOT>2.0.CO;2.

Vitart, F. “Impact of the Madden Julian Oscillation on Tropical Storms and Risk of Landfall in the ECMWF Forecast System.” Geophysical Research Letters 36, no. 15 (2009). https://doi.org/10.1029/2009GL039089.

Wheeler, Matthew C., and Harry H. Hendon. “An All-Season Real-Time Multivariate MJO Index: Development of an Index for Monitoring and Prediction.” Monthly Weather Review 132, no. 8 (August 1, 2004): 1917–32. https://doi.org/10.1175/1520-0493(2004)132<1917:AARMMI>2.0.CO;2.

Zhao, Chen, and Tim Li. “Basin Dependence of the MJO Modulating Tropical Cyclone Genesis.” Climate Dynamics 52, no. 9 (May 1, 2019): 6081–96. https://doi.org/10.1007/s00382-018-4502-y.

BIOGRAPHY

Jacob Campbell graduated with his Bachelor of Science for Mechanical Engineering from Trinity University in 2011. He was employed in various industries for several years until making the switch to atmospheric science in 2020 and receiving his Master of Science in Climate Science from George Mason University in 2022.